BNL-41996
Informal Report

3-D NUMERICAL ANALYSIS OF A HIGH-GAIN FREE-ELECTRON LASER

Juan C. Gallardo

October 19, 1988

CENTER FOR ACCELERATOR PHYSICS

BROOKHAVEN NATIONAL LABORATORY
ASSOCIATED UNIVERSITIES, INC.

Under Contract No. DE-AC02-76CH00016 with the

UNITED STATES DEPARTMENT OF ENERGY

BNL-41996
Informal Report

3-D NUMERICAL ANALYSIS OF A HIGH-GAIN FREE-ELECTRON LASER

BNL--41996

DE89 006981

Juan C. Gallardo

Brookhaven National Laboratory
Upton, New York 11973

ABSTRACT

We present a novel approach to the 3-dimensional high-gain free-electron laser amplifier problem. The method allows us to write the laser field as an integral equation which can be efficiently and accurately evaluated on a small computer. The model is general enough to allow the inclusion of various initial electron beam distributions to study the gain reduction mechanism and its dependence on the physical parameters.

This manuscript has been authored under contract number DE-ACO2-76-CH00016 with the U.S. Department of Energy. Accordingly, the U.S. Government retains a non-exclusive, royalty-free license to publish or reproduce the published form of this contribution, or allow others to do so, for U.S. Government purposes.

I. INTRODUCTION

Reported here is the progress of determining the e^- beam quality and undulator requirements needed to drive a free-electron laser(FEL) in the amplified spontaneous emission (ASE) model. Of particular importance toward this goal is the development of simple and inexpensive computer codes to simulate 3-D FEL physics. The feasibility of such a device and the likely power levels to be achieved critically depends on the presence of optical guiding, induced by high gain[1], and on proper modeling of the inhomogeneity of the electron pulse. The inhomogeneity is introduced by the initial distribution in phase space, i.e, energy spread, initial radius and emittance.

Since a complete simulation of the problem requires a large amount of computer CPU time, we will restrict ourselves to describing the laser field evolution, as it traverses the undulator, in the weak field regime below saturation.

The electron trajectories are determined by solving the Lorentz equations; these trajectories in turn are used to calculate the transverse current function, the non-linear driving source term in Maxwell's equation. The elliptical wave equation becomes a parabolic paraxial equation if we assume the slow wave amplitude and phase approximation. The evolution of the radiation field is obtained by solving this equation, formally equivalent to a 2-D time dependent Schrödinger-like equation[2]. There are two basic approaches to numerically compute the amplitude and phase of the laser wave. In the first approach, we expand the optical field in terms of orthonormal Gaussian modes (free space modes) so that our evolution equation is reduced to a system of differential equations for the time dependent coefficients of the expansion[3]. In the second approach, we express the field in the discrete space-time domain and evaluate the wave at the grid points of a mesh in the transverse coordinates[2] at each time step $\Delta\tau$.

In this work we use the latter method. An argument used against this approach has been the extensive computer CPU time required to achieve reasonable accuracy. It is known[4] that if we restrict ourselves to the weak signal regime, we can linearize the laser field equation and obtain an integral equation which, as we will show later, reduces to a convolution product in the transverse coordinates. This allows for an efficient and fast computation of the integral equation using standard Fast-Fourier Transform (FFT) routines[5].

As pointed out by Colson [2] it is convenient to normalize the x and y coordinates, $\frac{k}{2L}x^2 \rightarrow x^2$, $\frac{k}{2L}y^2 \rightarrow y^2$. $L = N\lambda_0$ is the length of the undulator, where λ_0 is the wavelength of the periodic magnetic field. The diffraction characteristics of the radiation in free space is determined by the free-space Green function

$$G(\vec{x}_\perp|\tau) = \frac{e^{i\frac{|\vec{x}_\perp|^2}{\tau}}}{\tau}\Theta(\tau) \tag{1}$$

with $\tau = \frac{ct}{L}$ the time variable normalized to the length of the undulator. A numerically stable solution[5] is obtained if $\frac{(\Delta\vec{x}_\perp)^2}{\Delta\tau} \approx 1$. We also see from the Green function that the diffraction effects are important when the electron beam radius r_e and the laser waist ω_0 are smaller than $\sqrt{\frac{\lambda L}{\pi}}$, i.e

$$r_e^2 \lesssim \frac{\lambda L}{\pi} \quad , \quad \omega_0^2 \lesssim \frac{\lambda L}{\pi}. \tag{2}$$

Our numerical code assumes an FEL in the high gain regime and a very small but coherent input wave. Its amplitude is approximately given by the spontaneous emission power emitted by the electron pulse in a gain length L_G (see next section). We also neglect the short pulse effects as the condition $\frac{N\lambda}{\sigma_z} \ll 1$, i.e. the slippage distance[6] ($s = N\lambda$) is smaller than the longitudinal length of the e^- pulse (σ_z).

I.a Electron Beam Quality

The bunching of the electron beam over the length of the undulator must be maintained for extracting energy from it. Clearly, for a non-perfect e^- beam with energy spread, angular spread, transverse emittance, and finite radius, the condition for maintaining appropriate matching between electron, laser light, and undulator is more difficult to achieve and, in general, there is a degradation of the gain of the device.

The natural width of the gain curve for a perfect e^- beam depends on the value of j (or equivalently ρ). The FEL parameter ρ, defined by Bonifacio et al. in Ref. 7, is widely used in the literature. To aid the reader we include in square brackets the most important formulas of this work in terms of this parameter. Any additional broadening induced by a realistic e^- beam is compared to the natural width in order to assess its degrading effects.

In our model calculation the properties of the e$^-$ beam are manifest in two equally important ways. First, the normalized current

$$j = 8N\frac{(e\pi KL)^2}{\gamma^3 mc^2}\hat{n} \tag{3}$$

is defined in terms of the particle density $\hat{n}$, the undulator parameter K and the length of the undulator $L = N\lambda_0$. This parameter describes the macroscopic properties of the e$^-$ beam. The electron beam is described in real space by a normalized distribution function $f(\vec{x}_\perp, z)$ which we assume to be written as the product of uncorrelated distribution functions

$$f(\vec{x}_\perp, z) = \frac{j_1(\vec{x}_\perp)\, j_2(z)}{(2\pi)^{\frac{3}{2}}\sigma_\perp^2 \sigma_z} \tag{4}$$

where σ_i $(i = \perp, z)$ is the standard (rms) deviation.

In terms of the total number of particles $\mathcal{N}$ in each micropulse of length $c\tau_e \approx 2\sigma_z$ we write the particle density as

$$\hat{n} = \frac{\mathcal{N}}{(2\pi)^{\frac{3}{2}}\sigma_\perp^2 \sigma_z} j_1(\vec{x}_\perp)\, j_2(z)$$

For a cylindrically symmetric e$^-$ beam of initial radius $r_e(\eta)$ and angular divergence $\Delta\theta$, we have $(0 \le \eta, \tau \le 1)$

$$\sigma_\perp^2 \equiv r_e(\tau)^2 = r_e(\eta)^2 + L^2(\tau - \eta)^2 \frac{r_e(\eta)^2}{(\beta^*)^2} \tag{5}$$

where η is the position of the waist, L is the length of the interaction region (undulator) and β^* is the focusing function.

Our analysis is valid in the long pulse limit, i.e. $\sigma_z >> N\lambda$, therefore, it is a good approximation to take a constant distribution in z, $j_2(z) = 1$. Substituting in Eq. (3) we obtain

$$\begin{aligned} j =& 8N\frac{(e\pi KL)^2}{\gamma^3 mc^2}\frac{2I}{ec(2\pi)^{\frac{1}{2}}}\frac{j_1(\vec{x}_\perp)}{\pi r_e(\tau)^2} = j_0 j_1(\vec{x}_\perp) \\ &\left[\rho = \frac{1}{4\pi N}\left(\frac{j_0}{2}\right)^{\frac{1}{3}}\right] \end{aligned} \tag{6}$$

where we used the peak current $I = \frac{ec\mathcal{N}}{2\sigma_z}$.

Introducing the normalized emittance of the beam $\epsilon_n = \gamma\epsilon = \gamma r_e(\eta)\,\Delta\theta$ we write

$$(\Delta\theta)^2 = \frac{\epsilon_n}{\beta^*\gamma} \quad \text{and} \quad r_e(\eta)^2 = \frac{\epsilon_n\beta^*}{\gamma}. \tag{7}$$

For a fixed emittance and particle energy the peak current I and consequently j (or equivalently ρ) increases as the focusing function β^* decreases.

Second, the source of the wave equation is $\left\langle \frac{e^{i\zeta(\vec{x}_\perp,\tau)}}{\gamma} \right\rangle_{\zeta_0,\nu_0}$, an average over the initial phase and phase velocity of sample electrons contained in a wavelength λ (microscopic scale). The definitions of phase and phase velocity are given in the next section. The average is written as $\langle \ldots \rangle \equiv \int_0^{2\pi} d\zeta_0 \int_{-\infty}^{\infty} d\nu_0 f_1(\zeta_0)\, f_2(\nu_0) \ldots$ where $f_1(\zeta_0)$ represents a uniform distribution of the phase (i.e. electrons are uniformly distributed in the longitudinal direction); $f_2(\nu_0)$ is a distribution of the phase velocity ν_0 produced by energy spread $\frac{\Delta\gamma}{\gamma}$, angular spread $\Delta\theta$, and transverse emittance.

In general this average tends to degrade the gain if the deviation in resonance parameter from the filamentary perfect e$^-$ beam is larger than a characteristic quantity σ (rms deviation) which depends on the inhomogeneity of the e$^-$ beam expressed in terms of ν_0. The characteristic rms deviation σ_E due to energy spread $\frac{\Delta\gamma}{\gamma}$ in the resonance parameter space is

$$\sigma_E = \frac{4\pi N}{\beta_{res}^2\,(1+K^2)}\frac{\Delta\gamma}{\gamma}, \tag{8}$$

The above expression is obtained using the energy definition and the resonance condition $\beta_{res} = \frac{k}{k+k_0}$ (see next section).

Any finite e$^-$ beam radius induces a dispersion in the resonance parameter. In a helical undulator the energy of an electron following a helical trajectory is a constant of motion; from $\frac{d\gamma}{d\tau} = 0$ we can write $\left(\Delta\beta_x^2 + \Delta\beta_y^2\right) = -\beta_z\Delta\beta_z$ and $\Delta\nu = -\frac{L(k+k_0)}{\beta_{res}}\left(\Delta\beta_x^2 + \Delta\beta_y^2\right)$. We show later that the equation of motion in the transverse plane $\vec{x}_\perp \equiv (x, y)$ for the corrections to the helical orbit are

$$\frac{d^2x}{d\tau^2} = -\omega_b^2 x \quad , \quad \frac{d^2y}{d\tau^2} = -\omega_b^2 y \tag{9}$$

where the betatron frequency is $\omega_b = \frac{Kk_0}{\gamma\sqrt{2}}L$. Conservation of energy in this harmonic motion leads to the relation

$$\left(\Delta\beta_x^2 + \Delta\beta_y^2\right) = \left(\frac{\omega_b}{L}\right)^2 \left[x(0)^2 + y(0)^2\right] + \left(\Delta\theta_x^2 + \Delta\theta_y^2\right), \tag{10}$$

and the rms deviation in resonance parameter due to betatron oscillations is

$$\sigma_b = \frac{4\pi N}{\beta_{res}^2(1+K^2)}\left[\tfrac{1}{2}K^2k_0^2\left(x(0)^2+y(0)^2\right)+\gamma^2\left(\Delta\theta_x^2+\Delta\theta_y^2\right)\right].$$

The geometrical emittance at the entrance of the undulator is $\epsilon_x = \Delta\theta_x x(0) \approx \epsilon_y \equiv \epsilon$. Assuming both terms in σ_b approximately equals using Eq. (7) we obtain $\beta^* = \frac{1}{\omega_b} = \frac{\sqrt{2}\gamma}{Kk_0}$ which is the natural undulator focusing. Therefore,

$$\sigma_b = \frac{4\pi N}{(1+K^2)\beta_{res}^2}\left[\tfrac{1}{2}K^2k_0^2\frac{\epsilon_n\beta^*}{\gamma}+\frac{\gamma\epsilon_n}{\beta^*}\right] \tag{11}$$

Both terms in the above formula have different behavior with β^*. However, a cursory look at j in Eq. (3) suggests that decreasing β^* increases the current parameter and consequently the power gain. On the other hand, for constant transverse emittance any decrease in β^* results in larger $\Delta\theta_x$ (i.e. larger σ_θ) with the corresponding degradation of the gain. The constraint on σ_θ is expressed by requiring that the different spreads in resonance parameter be smaller or comparable to the gain bandwidth[2]

$$\sigma_E\,,\,\sigma_\theta\,,\,\sigma_b \lesssim \sigma_\nu. \tag{12}$$

We estimate the width of the gain curve in the high gain regime by using the following arguments. The laser evolution equation can be cast in the form of the well known cubic equation $\alpha^3 - i\nu_0\alpha^2 - \frac{1}{2}ij_0 = 0$, assuming $a(\tau) = e^{i(\nu_0+\alpha)\tau}$. At resonance ($\nu_0 = 0$) the fastest growing root is $\alpha_0 \approx \frac{1}{2}\sqrt{3}\left(\frac{j_0}{2}\right)^{\frac{1}{3}}$ for $j_0 >> 1$. Substituting $\alpha \approx \alpha_0 + \alpha_1\nu_0 + \alpha_2\nu_0^2 + \ldots$ and after a simple algebra, $\alpha_1 = \frac{i}{2}$, $\alpha_2 = \frac{1}{9\alpha_0}$ and consequently, the gain becomes $G \approx \frac{1}{9}\exp\left(2\alpha_0 - \frac{2}{9\alpha_0}\nu_0^2\right)$ with rms deviation

$$\sigma_\nu \approx 1.76 j_0^{\frac{1}{6}} \qquad \left[= 1.76\sqrt{2^{\frac{7}{3}}\pi N\sqrt{\rho}}\right] \tag{13}$$

showing that the bandwidth in the high gain regime is significantly different from the low-gain bandwidth $\sigma_\nu \approx \pi$.

I.b Optical Guiding

We turn now to the condition of optical guiding[1]. For very high currents j $[\rho] >> 1$, the phase front of the laser radiation is significantly perturbed in the region where the electron beam overlaps the light. This phenomenon is known as *gain guiding* and arises from the fact that the e^- beam is the gain medium for the FEL. In addition, the FEL interaction tends to curve the laser wave fronts in the opposite direction of natural diffraction; as a result, spreading of the wave is cancelled and actual focusing of the generated coherent light[8] takes place. This is known as *refractive optical guiding.* We include also, *bending*[9] of the laser beam which is the physical consequence of trapping the laser radiation by the high gain medium, the e^- beam. An off-axis e^- beam leads to an off-axis laser beam. In the high gain regime all these effects cannot be separated; however, their relative importance depends on the current j, the transverse dimensions r_e and transverse profile of the e^- beam, and the resonance parameter ν_0. Optical guiding is of paramount importance for high gain (ASE) amplifiers where long undulators are needed to achieve saturation. The natural diffraction of the wave conspires to reduce the achievable laser power by means of early weak saturation i.e., the coherent radiation generated by the e^- beam in the distance z_R exactly compensates for the weakening of the wave on axis due to diffraction $\frac{E_0}{\omega(z)^2}$. However, the optical guiding phenomena confines the light beam in the region of the e^- beam and allows a continuous interaction over many Rayleigh lengths z_R (or more appropriately over many gain lengths L_G)[10]. The characteristic Gaussian divergence z_R of light emitted by a source of transverse dimensions equal to the e^- beam radius r_e is given by $z_R = \frac{\pi r_e^2}{\lambda}$. The gain length L_G is defined as the distance in the undulator where the radiation will be e-folded ,

$$L_G = \left[\frac{\sqrt{3}}{2}\left(\frac{j}{2}\right)^{\frac{1}{3}}\right]^{-1} \lambda_0 N \qquad \left[= \frac{\lambda_0}{2\pi\rho\sqrt{3}}\right]. \tag{14}$$

To continuously compensate for the phase shift due to *free-field* diffraction we impose

$$\frac{\pi r_e^2}{\lambda} \gtrsim \frac{2\lambda_0 N \left(\frac{j}{2}\right)^{-\frac{1}{3}}}{\sqrt{3}} \qquad \left[\frac{2\lambda_0}{\sqrt{3}}\frac{1}{4\pi\rho}\right]. \tag{15}$$

II. THEORETICAL ANALYSIS

An FEL uses a beam of relativistic e^- passing through a long transverse, periodic magnetic field (undulator) to amplify a copropagating optical wave. The electron dynamics is described by the Lorentz equation; the Maxwell wave equation, driven by a single-particle e^- current, governs the wave dynamics. We present a description of the system electron-laser dynamics following a well-established formalism in the space-time domain. Colson [2] has published a comprehensive and complete review of the theory and its generalizations to include the inhomogeneity of the electron beam. We summarize below the main equations for a free electron laser *á la Colson* and refer the reader to Ref. 2 for more details.

II.a Electron Dynamics

To compute the electron trajectories in the interaction region where both undulator and laser fields coexist, we solve the Lorentz force equation. The helical undulator field near the axis is given by,

$$\begin{aligned}\vec{B} \approx B_0\Big(& [1+\frac{1}{8}k_0^2(3x^2+y^2)]\cos k_0 z - \frac{1}{4}k_0^2 xy \sin k_0 z\,, \\ & [1+\frac{1}{8}k_0^2(x^2+3y^2)]\sin k_0 z + \frac{1}{4}k_0^2 xy \cos k_0 z\,, \\ & -[1+\frac{1}{8}k_0^2(x^2+y^2)][x \sin k_0 z - y \sin k_0 z]\Big)\end{aligned} \tag{16}$$

and the optical field is described by

$$\vec{E} = E(\vec{x}_\perp,t)\Big(\cos(kz-\omega t+\phi(\vec{x}_\perp,t))\,,\ -\sin(kz-\omega t+\phi(\vec{x}_\perp,t))\,,\ 0\Big),$$

where $\lambda = \frac{2\pi c}{\omega}$ is the carrier wavelength. We assume the customary slow-phase and amplitude approximation, i.e., $E(\vec{x}_\perp,t)$ and $\phi(\vec{x}_\perp,t)$ are slowly varying functions of time t ($E' >> E''$ and $\phi' >> \phi''$). Here, E' stands for the time derivative. The transverse velocity $\vec{\beta}_\perp$ is derived from the Lorentz equation, obtaining on axis

$$\gamma\vec{\beta}_\perp = -K(\cos k_0 z\,,\ \sin k_0 z\,,\ 0)$$

where we have neglected terms proportional to $\lambda E << \lambda_0 B_0$. The undulator parameter is $K = \frac{eB}{mc^2 k_0}$. The correction to the helical orbit leads, after an average over λ_0, to harmonic equations for the transverse coordinates with frequency of oscillation given by $\omega_b^2 = \frac{1}{2}\left(\frac{Kk_0L}{\gamma}\right)^2$. The orbits are

$$x(\tau) \approx x(0)\cos\omega_b\tau + \frac{\dot{x}(0)}{\omega_b}\sin\omega_b\tau \tag{17a}$$

$$y(\tau) \approx y(0)\cos\omega_b\tau + \frac{\dot{y}(0)}{\omega_b}\sin\omega_b\tau \tag{17b}$$

with initial conditions $x(0)$, $y(0)$, $\dot{x}(0) = L\theta_x$ and $\dot{y}(0) = L\theta_y$.

The fourth component of the Lorentz force gives the electron energy change

$$\frac{d\gamma}{d\tau} = \frac{\tilde{K}KkL}{\gamma}\cos\left[(k+k_0)z - Lk\tau + \phi\right] \tag{18}$$

with $\tilde{K} = \frac{eE\lambda}{2\pi mc^2}$. The value of the phase $(k+k_0)z - \omega t + \phi(\vec{x}_\perp, t)$ determines the decrease or increase of the electron energy and consequently, by energy conservation, the increase (gain) or decrease (particle acceleration) of the radiation field energy. The normalized longitudinal velocity is recovered from the electron energy definition $\gamma^{-2} = 1 - \left(\frac{K}{\gamma}\right)^2 - \beta_z^2$. These expressions suggest a useful formalism to describe the electron dynamics in the combined undulator and laser fields; we introduce the electron phase $\zeta(\vec{x}_\perp, \tau) = (k+k_0)z - Lk\tau$ and the phase velocity $\nu(\vec{x}_\perp, \tau) \equiv \frac{d\zeta}{d\tau} = L(k+k_0)\beta_z - Lk$, where $\tau = \frac{ct}{L}$ is the normalized time variable. The resonance condition is obtained by imposing the condition $\nu = 0$, i.e., $\beta_z^{res} = \frac{k}{k+k_0}$ which corresponds to the stationary phase in Eq. (18). Combining $\dot{\beta}_z$ and $\dot{\nu}$ we can write (the dot denotes τ derivative)

$$\begin{aligned} \dot{\nu}(\vec{x}_\perp, \tau) &= \mathrm{Re}\left\{a(\vec{x}_\perp, \tau)\, e^{i\zeta(\vec{x}_\perp, \tau)}\right\} \\ \dot{\zeta}(\vec{x}_\perp, \tau) &= \nu(\vec{x}_\perp, \tau) \end{aligned} \tag{19}$$

where $a(\vec{x}_\perp, \tau)$ is the slowly varying dimensionless complex laser field defined as

$$a(\vec{x}_\perp, \tau) = \frac{8\pi e K N^2 \lambda_0}{mc^2\gamma^2} \frac{E(\vec{x}_\perp, \tau)}{\left(1 - \frac{(1+K^2)}{\gamma^2}\right)}. \tag{20}$$

II.b Wave Dynamics

The optical field is governed by the wave equation, which in the slow wave and phase approximation reads[2]

$$\left(-\frac{i}{4}\nabla_\perp^2 + \frac{\partial}{\partial\tau}\right)a(\vec{x}_\perp,\tau) = -j(\vec{x}_\perp,\tau)\left\langle e^{-i\zeta(\vec{x}_\perp,\tau)}\right\rangle_{\zeta_0,\nu_0}, \tag{21}$$

where $j\left(\vec{x}_\perp,\tau\right)$ is the current parameter defined in (6) and $<\ \ldots\ >_{\zeta_0,\nu_0}$ represents an average over the initial phase and phase velocity of the electrons in a section of the beam of length λ, the carrier wavelength. The transverse coordinate $\vec{x}_\perp$ is normalized as indicated in the Introduction.

The coupled system of Eq. (19) and Eq. (21) describes simply and accurately the physics of the FEL interaction. We have not included in these equations a factor $\left(1 - \frac{\nu}{2\pi N}\right)$ which is close to 1 unless the electrons lose an appreciable amount of energy during the interaction. We also note that this coupled system of Eqs. satisfies energy conservation[11].

It is useful to define $\zeta\left(\vec{x}_\perp,\tau\right) = \zeta_0 + \nu_0\tau + \delta\zeta\left(\vec{x}_\perp,\tau\right)$ and $\nu\left(\vec{x}_\perp,\tau\right) = \frac{d}{d\tau}\delta\zeta\left(\vec{x}_\perp,\tau\right)$. A formal solution of Eq. (19) is

$$\delta\zeta\left(\vec{x}_\perp,\tau\right) = \int_0^\tau d\tau'\left(\tau-\tau'\right)\mathrm{Re}\left\{a\left(\vec{x}_\perp,\tau'\right)e^{i\zeta_0+i\nu_0\tau'+i\delta\zeta(\vec{x}_\perp,\tau')}\right\} \tag{22}$$

In the weak field regime we neglect $\delta\zeta$ in the above equation and keep first order terms in Eq. (21) to obtain,

$$\left(-\frac{i}{4}\nabla_\perp^2 + \frac{\partial}{\partial\tau}\right)a(\vec{x}_\perp,\tau) = \frac{ij(\vec{x}_\perp,\tau)}{2}\left\langle\int_0^\tau d\tau'(\tau-\tau')e^{-i\nu_0(\tau-\tau')}a(\vec{x}_\perp,\tau')\right\rangle_{\nu_0} \tag{23}$$

still to be computed is the average over the distribution of phase velocities induced by the inhomogeneities of the electron beam, i.e., energy spread, emittance, betatron oscillations and finite transverse dimensions. For Gaussian or Lorenztian distributions the average over ν_0 in the right-hand side of Eq. (23) can be performed analytically; we obtain

$$\left(-\frac{i}{4}\nabla_\perp^2 + \frac{\partial}{\partial\tau}\right)a(\vec{x}_\perp,\tau) = \tfrac{1}{2}ij_0j_1(\vec{x}_\perp)\int_0^\tau d\tau'(\tau-\tau')e^{-i\nu_0(\tau-\tau')}a(\vec{x}_\perp,\tau') \times F(\sigma_E,\sigma_\theta,\sigma_b,\tau-\tau') \tag{24}$$

where

$$F\left(\sigma_E,\sigma_\theta,\sigma_b,\tau-\tau'\right) = \frac{e^{-\frac{1}{2}\sigma_E^2(\tau-\tau')^2}}{\left[1-i\sigma_\theta\left(\tau-\tau'\right)\right]\left[1-i\sigma_b\left(\tau-\tau'\right)\right]}$$

represents the correction term due to inhomogeneities of the e$^-$ beam. σ_E , σ_θ , σ_b are the rms deviations defined in Eqs.(8), (9) and (12). We have also written the current parameter as the product of a constant j_0, dependent only on the peak current, and $j_2(\vec{x}_\perp)$, which contains all the transverse dependence.

Making use of the Green function theorem[12], a formal solution of Eq. (24) can be written as

$$a(\vec{x}_\perp,\tau) = \int_0^\tau d\tau' \int d\vec{y}_\perp G(\vec{x}_\perp - \vec{y}_\perp|\tau-\tau')\, S(\vec{y}_\perp,\tau') - \frac{i}{\pi}\int d\vec{y}_\perp G(\vec{x}_\perp - \vec{y}_\perp|\tau)\, a(\vec{y}_\perp,0) \tag{25}$$

where $G(\vec{x}_\perp - \vec{y}_\perp|\tau-\tau')$ given in Eq.1 is the Green function[13] for the free-particle Schrödinger-like equation

$$\left(\nabla_\perp^2 + 4i\frac{\partial}{\partial\tau}\right) G(\vec{x}_\perp - \vec{y}_\perp|\tau-\tau') = -4\pi\delta(\vec{x}_\perp - \vec{y}_\perp)\,\delta(\tau-\tau'),$$

and the *source term* or *potential* is

$$S(\vec{x}_\perp,\tau) = \frac{1}{2}\frac{ij_0 j(\vec{x}_\perp)}{\pi}\int_0^\tau d\tau'\,(\tau-\tau')\,e^{-i\nu_0(\tau-\tau')}a(\vec{x}_\perp,\tau)\,F(\sigma_E,\sigma_\theta,\sigma_b,\tau-\tau').$$

The laser field at time step n ($\tau = n\Delta$) is expressed in terms of the values of the field at all previous time steps and is efficiently computed by working in the Fourier space. In the numerical implementation, we make use of the fast Fourier transform (FFT) and note that the *source term* consists of a convolution product which leads to

$$FFT\Big[\int d\vec{y}_\perp G(\vec{x}_\perp - \vec{y}_\perp|\tau-\tau')j_1(\vec{y}_\perp)a(\vec{y}_\perp,\tau')\Big] = FFT\Big[G(\vec{x}_\perp|\tau-\tau')\Big] \times FFT\Big[j_1(\vec{x}_\perp)a(\vec{x}_\perp,\tau')\Big] \tag{26}$$

where the Fourier transform of the Green function, a Gaussian function, is performed analytically and therefore does not add to the cpu time needed for the problem. We also note that if the initial laser field is a fundamental Gaussian mode with a waist at the beginning of the undulator, the second term in Eq. (25) is analytically computed. The diffractive Gaussian beam of dimensionless waist ω_0 and physical Rayleigh range $z_R = \frac{\pi\omega_0^2}{\lambda}$ at time τ is of the form, $\frac{e^{-\frac{|\vec{x}_\perp|^2}{(\omega_0^2+i\tau)}}}{\omega_0^2+i\tau}$.

The first term in Eq. (25) contains the current $j_2(\vec{x}_\perp)$ and is the factor we numerically evaluate in a rectangular mesh of 32×32 points. Typically, we compute the convolution product in 50 time steps. After multiplying the Green function transform by $FFT\Big[j_1(\vec{x}_\perp)a(\vec{x}_\perp,\tau')\Big]$ we perform the anti-transform $FFT^{-1}\Big[\ldots\Big]$ and then we perform the numerical time integration (note that at $\tau' = \tau$ the integrand vanishes) using a simple Simpson subroutine with accuracy $(\Delta\vec{x}_\perp)^5$. The above function is added to the free-diffractive input Gaussian wave to obtain the laser field at time $\tau = n\Delta$ at each point of the chosen rectangular mesh in the transverse plane.

The transverse profile of the current function $j_1(\vec{x}_\perp)$ is arbitrary in the theory; we have considered three different distributions:

a) Gaussian

$$j_1(\vec{x}_\perp) = e^{-\frac{|\vec{x}_\perp|^2}{r_e^2}} \tag{27a}$$

b) parabolic

$$j_1(\vec{x}_\perp) = \begin{cases} 2(1-\frac{|\vec{x}_\perp|^2}{r_e^2}) & |\vec{x}_\perp| \lesssim r_e \\ 0 & |\vec{x}_\perp| > r_e \end{cases} \tag{27b}$$

c) step function

$$j_1(\vec{x}_\perp) = \begin{cases} 1 & |\vec{x}_\perp| \lesssim r_e \\ 0 & |\vec{x}_\perp| > r_e \end{cases} \tag{27c}$$

To simulate an FEL in the ASE regime we start with a very small coherent input field; of course, the gain of the device is independent of this initial wave field. At the end of the undulator the laser amplitude and mode content depend on the non-linear interaction between electrons, undulator magnetic field and the laser field described by the parameters j_0, $j_1(\vec{x}_\perp)$, r_e, σ_E, σ_θ and σ_b. The results of the calculation for different parameters are displayed in various figures.

III. SAMPLE RESULTS AND DISCUSSION

The set of parameters chosen as an example to illustrate the method proposed in this work are given in Table 1. For comparison we also give the result obtained using a 1-D theory[15]. This example corresponds to an FEL in the 30 nm wavelength range operating in the ASE mode. The e$^-$ beam has an rms bunch length of σ_e = 1ps, an energy spread $\frac{\Delta\gamma}{\gamma} = 0.1\%$, a normalized emittance $\epsilon_n = 4.2 \times 10^{-6}\,\mathrm{m-rad}$ and longitudinal brilliance[14]

$$B_L = \frac{e\mathcal{N}c}{\sqrt{2\pi}\epsilon_L} = \frac{I_p}{\delta\gamma} = 70\,\mathrm{A}.$$

To reach saturation in an ASE mode the length of the undulator is given by $N \approx \rho^{-1} \approx 10^3$. The undulator parameter K is taken to be 1. Fig. 1 is a typical example of the evolution of the amplitude of the laser field as it traverses the undulator. Fig. 2 displays the evolution of the phase of the wave subtracted from the input Gaussian quadratic phase

$$\phi(\vec{x}_\perp, \tau) = \frac{|\vec{x}_\perp|^2(\tau-\eta)}{\omega_0^4 + (\tau-\eta)^2} - \tan^{-1}\frac{(\tau-\eta)}{\omega_0^2} \tag{28}$$

where η is the position of the waist at $\tau = 0$.

The gain length coefficient L_G versus τ is plotted in Fig. 3 and the evolution of the $1/e$ width of the laser amplitude in Fig. 4. The gain length coefficient is defined as $L_G = \ln(G(\tau)+1)$ with

$$1 + G(\tau) = \frac{P(\tau)}{P(0)} \equiv e^{L_G\tau}. \tag{29}$$

To illustrate the optical guiding phenomena at this high gain regime we show in Figs. 5 - 8 the evolution of the laser field with an electron beam positioned off-axis at $x = 5$ and $y = 2$; the centroid of the laser field is coincident with that of the e$^-$ beam at the end of the undulator.

This model only describes the weak field regime and does not include saturation. Furthermore, the finite dimensions of the electron pulse in the longitudinal direction are neglected. The relevant parameter that quantifies the short-pulse effects is the coupling parameter $\mu_c = \frac{N\lambda}{\sigma_e} \ll 1$.

We have presented a simple model of the FEL interaction in an ASE mode and a selected sample of results. The development of the numerical code that solves the integral equation for the laser field, is carried out in dimensionless parameters and therefore is applied, in principle, to many different sets of electron beam and undulator parameters. We are continuing our effort to accurately model the physics of the FEL interaction; in particular we are examining the gain degradation effects introduced by an imperfect electron pulse. Simultaneously, we are working to optimize the numerical code to reduce its running time and benchmark its performance against analytical results[15] and existing 3-D codes[16].

Acknowledgements

I would like to thank the members of the Center for Accelerator Physics (CAP), in particular C. Pellegrini, H. Kirk, R. Fernow; and also Li-Hua Yu and S. Krinsky for many critical comments and contributions to this study. This research was supported in part by the U.S. Department of Energy under contract DE-ACO2-76-CH00016.

References

1. G. T. Moore, Nucl. Instrum. & Meth. A239, 19 (1985); J. M. Wang and L. H. Yu, Nucl. Instrum. & Meth. A250, 484 (1986); L. H. Yu and S. Krinsky, *Proc. Conference on Short Wavelength Radiation*, AIP Conf. Proc. No. 147, D. T. Atwood and J. Bokor Eds., American Institute of Physics, 1986; also first reference in Ref. 4; E. T. Scharlemann, A. M. Sessler and J. M. Wurtele, Phys. Rev. Lett. 54, 1925 (1985); G. T. Moore, Opt. Comm. 52, 46 (1984); C. M. Tang and P. A. Sprangle, IEEE J. Quantum Electron. QE-21, 970 (1985).

2. W. B. Colson and J. L. Richardson, Phys. Rev. Lett. 50, 1050 (1983); W. B. Colson, "Fundamental Free-Electron Laser Theory and New Principles for Advanced Devices", Proc. SPIE 738, 2 (1988); W. B. Colson and A. M. Sessler, Ann. Rev. Nucl. & Part. Sci. 35, 25 (1985); W. B. Colson and P. Elleaume, App. Phys. B29, 101 (1982); B. D. McVey, Nucl. Instrum. & Meth., A250, 449 (1986); W. B. Colson, Nucl. Instrum. & Meth., A237, 1 (1985).

3. P. Elleaume and D. A. G. Deacon, App. Phys. B33, 9 (1984); P. Elleaume and D. A. G. Deacon, SPIE. 453, 262 (1984); D. C. Quimby and J. Slater, IEEE J. Quantum Electron. QE-19, 800 (1983); B. J. Coffey, M. Lax and C. L. Elliot, IEEE J. Quantum Electron. QE-19, 297 (1983); P. Sprangle and C. -M. Tang, App. Phys. Lett. 39, 677 (1981); S. Prasad and G. T. Moore, Phys. Rev. A31, 343 (1985); L. R. Elias and J. C. Gallardo, Phys. Rev. A24, 3276 (1981); J. Goldstein, B. D. McVey and B. E. Newnam, SPIE 582, 350 (1986); E. T. Scharlermann et al., Nucl. Instrum. & Meth., A250, 150 (1986); S. Benson and J. M. J. Madey, Opt. Comm., 56, 212 (1985).

4. W. B. Colson, J. C. Gallardo and P. M. Bosco, Phys. Rev. A34, 4875 (1986); W. B. Colson and J. Blau, Nucl. Instrum. & Meth., A259, 198 (1987); second reference in Ref.7; J. C. Gallardo et al.,Phys. Rev. A36, 3222 (1987); J. C. Gallardo et al., Nucl. Instrum & Meth., Axxx, xxx (1988); W. B. Colson, Nucl. Instrum & Meth., Axxx, xxx (1988).

5. W. H. Press, B. P. Flannery, S. A. Teukolsky and W. T. Vetterling, *Numerical Recipes. The art of Scientific Computing*, Cambridge University Press, 1986, pp. 635.

6. W. B. Colson, Nucl. Instrum. & Meth., A237, 1 (1985); W. B. Colson and A. Renieri, J. Phys.(Paris), 44, C1-11 (1983); U. Bizarri et al., Riv. Nuovo Cimento, xxx, xxx (1988); G. Dattoli et al., Phys. Rev., A37, 4326 (1988).

7. Kwang-Je Kim, Phys. Rev. Lett. 57, 1871 (1986); R. Bonifacio, C. Pellegrini and L. M. Narducci, Opt. Comm. 50, 373 (1984); J. B. Murphy and C. Pellegrini, "Introduction to the Physics of the Free-Electron Laser", *Proc. of the Joint US-CERN Particle Accelerator School*, M. Month and S. Turner Eds., Springer Verlag, Lectures Notes in Physics (1988); J. B. Murphy and C. Pellegrini, J. Opt. Soc. Am. B2, 259 (1985); J. C. Goldstein, B. D. McVey and C. J. Elliott, "Conceptual designs of a 50 nm FEL oscillator and a $20-40\,nm$ SASE amplifier," *Proc. 9th International Free-Electron Laser Conference*, Williamsburg, Virginia (1987).

8. P. Sprangle, A. Ting and C. M. Tang, Phys. Rev. Lett. 59, 202 (1987); J. E. LaSala et al., Phys. Rev. Lett. 59, 2047 (1987).

9. R. W. Warren and B. D. McVey, Nucl. Instrum. & Meth. A259, 154 (1987); see also previous reference.

10. C. Pellegrini, Proceedings of the *9th International Free-Electron Laser Conference*, Williamsburg, Virginia, September 1987; J. C. Gallardo, R. Fernow, R. Palmer, C. Pellegrini, IEEE J. Quantum Electron. QE- 24, 1557, (1988); J.C. Goldstein, B.D. McVey, B.E. Newnam, Proc. SPIE 582, 350 (1987), R. Tatchyn and I. Lindau Eds.; J.L. Lasala, D. Deacon, J.M.J. Madey, Nucl. Instrum. & Meth. A250, 262 (1986); J. Gea-Banacloche, G.T. Moore, R.R. Schlicher, M.O. Scully, H. Walther, IEEE J. Quantum Electron. QE-23, 1558 (1987); J.M.J. Madey, AIP Conference Proc. No.118, 12, J.M.J. Madey and C. Pellegrini, Eds., NY: American Institute of Physics, 1984; J.B. Murphy, C. Pellegrini, Nucl. Instrum. & Meth. A237, 159 (1985); K.-J. Kim, J.J. Bisognano, A.A. Garren, K. Halbach, J.M. Peterson, Nucl. Instrum. & Meth. A239, 54 (1985); M. Billardon et.al., IEEE, J. Quantum Electron. QE-21, 805 (1985); J. Goldstein, T. Wang, B. McVey, B. Newnam, Proc. of the 1987 IEEE Particle Accelerators Conference, E. Lindstrom, Ed., Washington, D.C.; J. Ortega, et.al., IEEE

J. Quantum Electron. QE-21, 909 (1985); J.M.J. Madey and C. Pellegrini, Eds., *Free-Electron Generation of Extreme Ultraviolet Coherent Radiation*, AIP Conference Proceedings, No.118 NY: American Institute of Physics, 1984; J.B. Murphy and C. Pellegrini, Eds., *Proceedings of the ICFA Workshop on low emittance* $e^- - e^+$ *beams*, Brookhaven National Laboratory, New York, March 1987; B. Newnam, J. Goldstein, J. Fraser, AIP Conference Proceedings No.118, 190, J.M.J. Madey and C. Pellegrini Eds., NY: American Institute of Physics, 1984; R. Fernow, R. Palmer, C. Pellegrini, *Proposal for a pico-second pulsed x-ray source in the* $2-20$ *KeV region*, BNL Internal Report (1986); B. Kinkaid, J. Opt. Soc. Am. B2, 1294 (1985).

11. M. Xie, D. A. G. Deacon and J. M. J. Madey, Proceedings of the *9th International Free-Electron Laser Conference*, Williamsburg, Virginia, September 1987.
12. P. M. Morse and H. Feshbach, *Methods of Theoretical Physics*, pp. 857, McGraw-Hill Book Company, New York, 1953.
13. R. P. Feynman and A. R. Hibbs, *Quantum Mechanics and Path Integrals*, pp.42, McGraw-Hill Book Company, New York, 1965; J. J. Sakurai, *Modern Quantum Mechanics*, pp. 109, The Benjamin/Cummings Publishing Company, 1985.
14. J. B. Murphy and C. Pellegrini, Eds. Proceedings of the ICFA Workshop on Low Emittance e^+ - e^- beams, Brookhaven National Laboratory, NY, March 1987.
15. Li-Hua Yu and S. Krinsky, *Gain reduction due to betatron oscillations in a Free-Electron Laser*, submitted to Phys. Lett. A, 1988; also, *Betatron oscillations in a free-electron laser*, Proceedings of the *9th International Free-Electron Laser Conference*, Williamsburg, Virginia, September 1987; Li-Hua Yu and S. Krinsky, Phys. Rev., A35, 3406 (1987).
16. B. D. McVey, Nucl. Instrum. & Meth. A250, 449 (1986); E. T. Scharlemann et al., Nucl. Instrum. & Meth. A250, 150 (1986); J. Wurtele, private communication.

Figure Captions

Fig. 1: Transverse profile of the laser field amplitude at several position along the undulator corresponding to the parameters shown in Table 1. The initial Gaussian field has a beam waist ω_0 equal to electron beam radius r_e.

Fig. 2: Phase of the laser field minus the quadratic gaussian phase given in Eq. (28) at several position along the undulator corresponding to the parameters shown in Table 1.

Fig. 3: Evolution of the gain length coefficient L_G along the undulator.

Fig. 4: Evolution of the $1/e$ width of the laser amplitude along the undulator.

Fig. 5: Same as in Fig. 1 with an off-axis electron beam.

Fig. 6: Same as in Fig. 2 with an off-axis electron beam.

Fig. 7: Same as in Fig. 3 with an off-axis electron beam.

Fig. 8: Same as in Fig. 4 with an off-axis electron beam.

Table Captions

Table 1: Electron beam and undulator parameters used in the example shown in Fig. 1 - Fig. 8.

Energy [GeV]	0.76
σ_e [cm]	0.03
$\frac{\Delta\gamma}{\gamma}$ [%]	0.1
$\mu_c = \frac{N\lambda}{\sigma_e}$	4.0×10^{-6}
ϵ_n [m-rad]	4.2×10^{-6}
λ_0 [m]	0.03
L=Nλ_0 [m]	24.0
$\rho \times 10^3$	1.25
λ [nm]	33.3
L_G [m^{-1}] 1-D	12.56
3-D	20.9
R_{laser} [mm]	1.76×10^{-3}

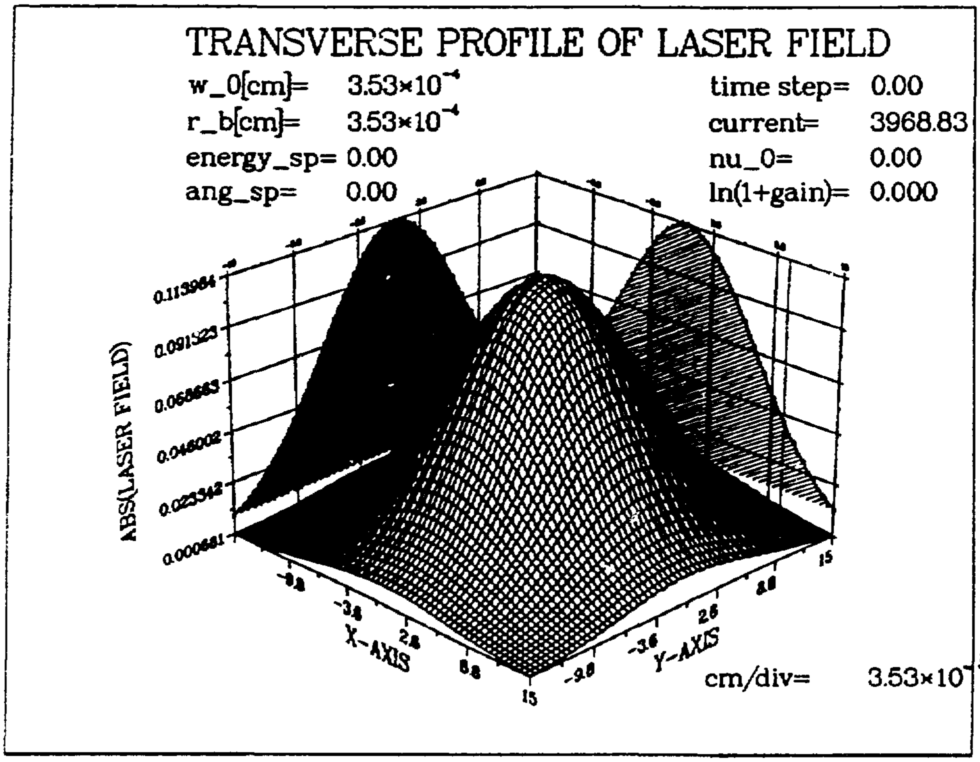
TRANSVERSE PROFILE OF LASER FIELD
w_0[cm]= 3.53×10⁻⁴
r_b[cm]= 3.53×10⁻⁴
energy_sp= 0.00
ang_sp= 0.00
time step= 0.00
current= 3968.83
nu_0= 0.00
ln(1+gain)= 0.000
ABS(LASER FIELD)
0.113984
0.091323
0.068663
0.046002
0.023342
0.000681
X-AXIS
Y-AXIS
-9.8
-3.6
2.6
8.8
15
cm/div= 3.53×10⁻⁵

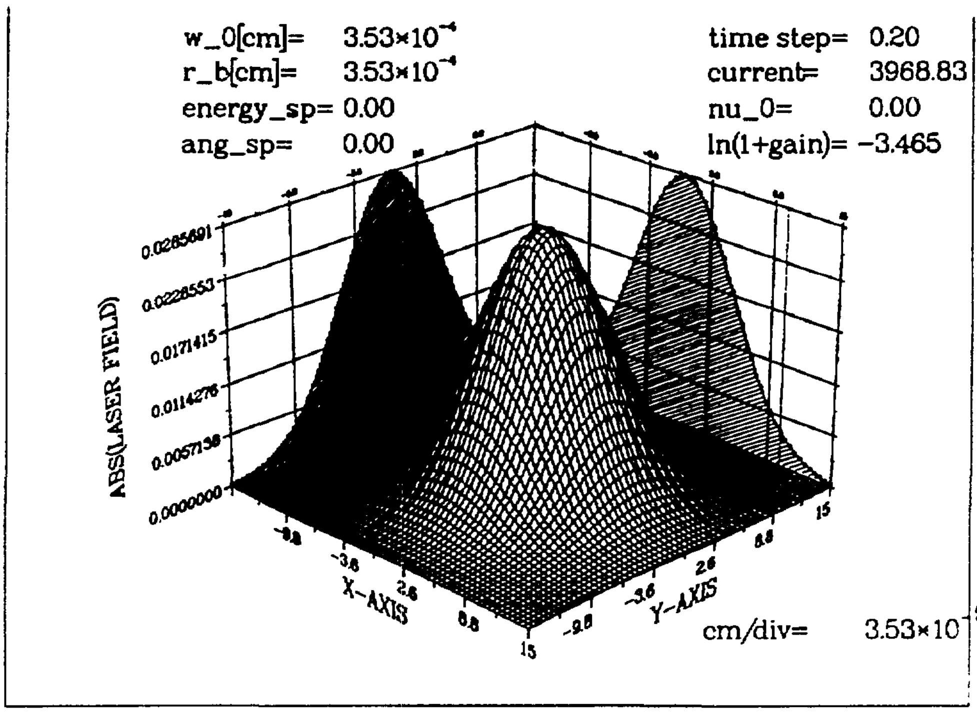
w_0[cm]= 3.53×10⁻⁴
r_b[cm]= 3.53×10⁻⁴
energy_sp= 0.00
ang_sp= 0.00
time step= 0.20
current= 3968.83
nu_0= 0.00
ln(1+gain)= −3.465
ABS(LASER FIELD)
0.0285691
0.0228553
0.0171415
0.0114276
0.0057138
0.0000000
X-AXIS
Y-AXIS
-9.8
-3.6
2.6
8.8
15
cm/div= 3.53×10⁻⁵

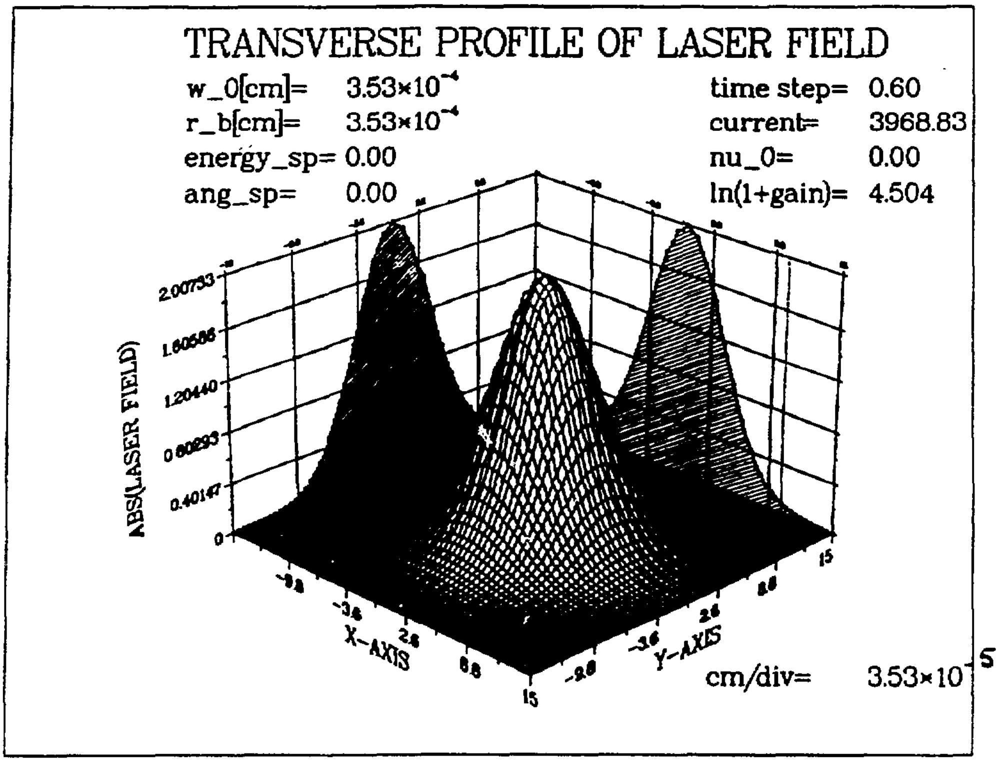
TRANSVERSE PROFILE OF LASER FIELD
w_0[cm]= 3.53×10^-4
r_b[cm]= 3.53×10^-4
energy_sp= 0.00
ang_sp= 0.00
time step= 0.60
current= 3968.83
nu_0= 0.00
ln(1+gain)= 4.504
ABS(LASER FIELD)
2.00733
1.60586
1.20440
0.80293
0.40147
0
-9.8
-3.6
2.6
8.8
15
X-AXIS
-9.8
-3.6
2.6
8.8
15
Y-AXIS
cm/div= 3.53×10^-5

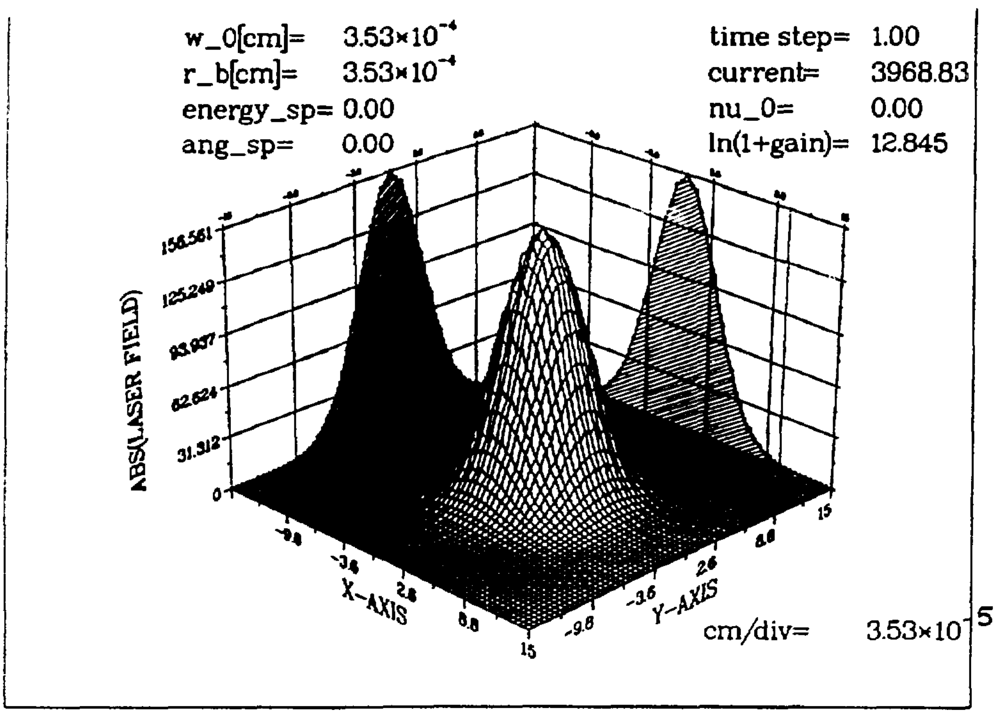
w_0[cm]= 3.53×10^-4
r_b[cm]= 3.53×10^-4
energy_sp= 0.00
ang_sp= 0.00
time step= 1.00
current= 3968.83
nu_0= 0.00
ln(1+gain)= 12.845
ABS(LASER FIELD)
156.561
125.249
93.937
62.624
31.312
0
-9.8
-3.6
2.6
8.8
15
X-AXIS
-9.8
-3.6
2.6
8.8
15
Y-AXIS
cm/div= 3.53×10^-5

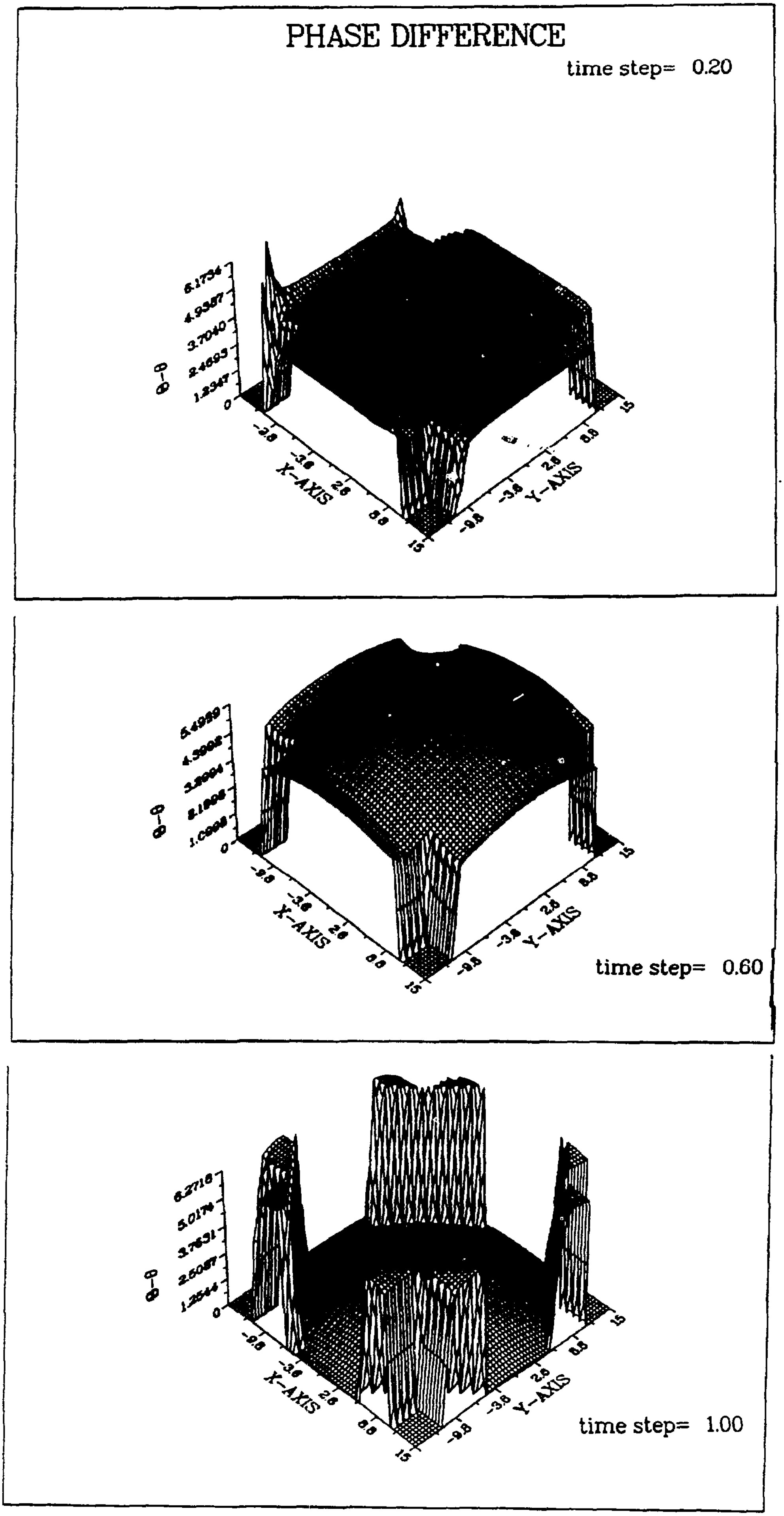
PHASE DIFFERENCE
time step= 0.20
X-AXIS
Y-AXIS
time step= 0.60
X-AXIS
Y-AXIS
time step= 1.00
X-AXIS
Y-AXIS

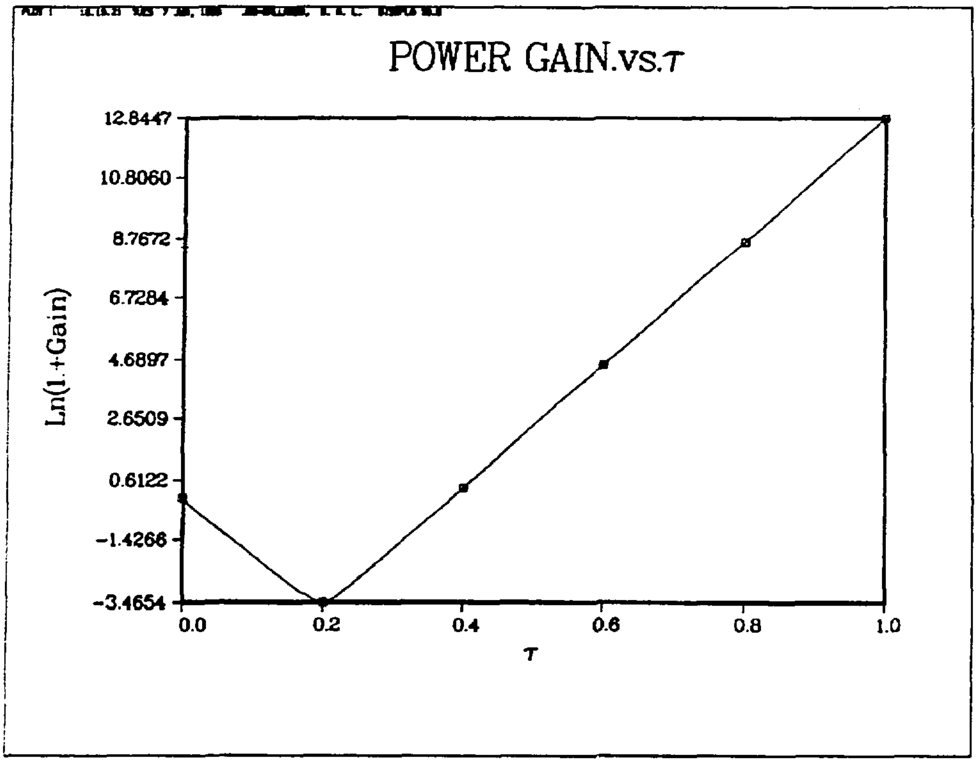
POWER GAIN.vs.τ
Ln(1.+Gain)
12.8447
10.8060
8.7672
6.7284
4.6897
2.6509
0.6122
-1.4266
-3.4654
0.0
0.2
0.4
0.6
0.8
1.0
τ

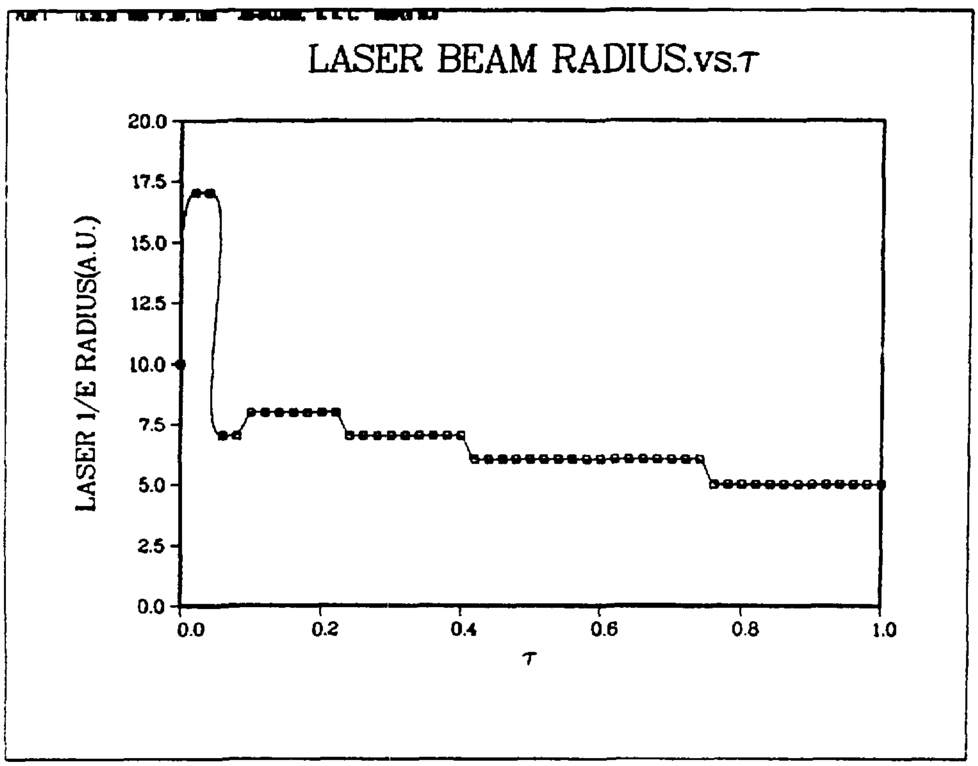
LASER BEAM RADIUS.vs.τ
LASER 1/E RADIUS(A.U.)
20.0
17.5
15.0
12.5
10.0
7.5
5.0
2.5
0.0
0.0
0.2
0.4
0.6
0.8
1.0
τ

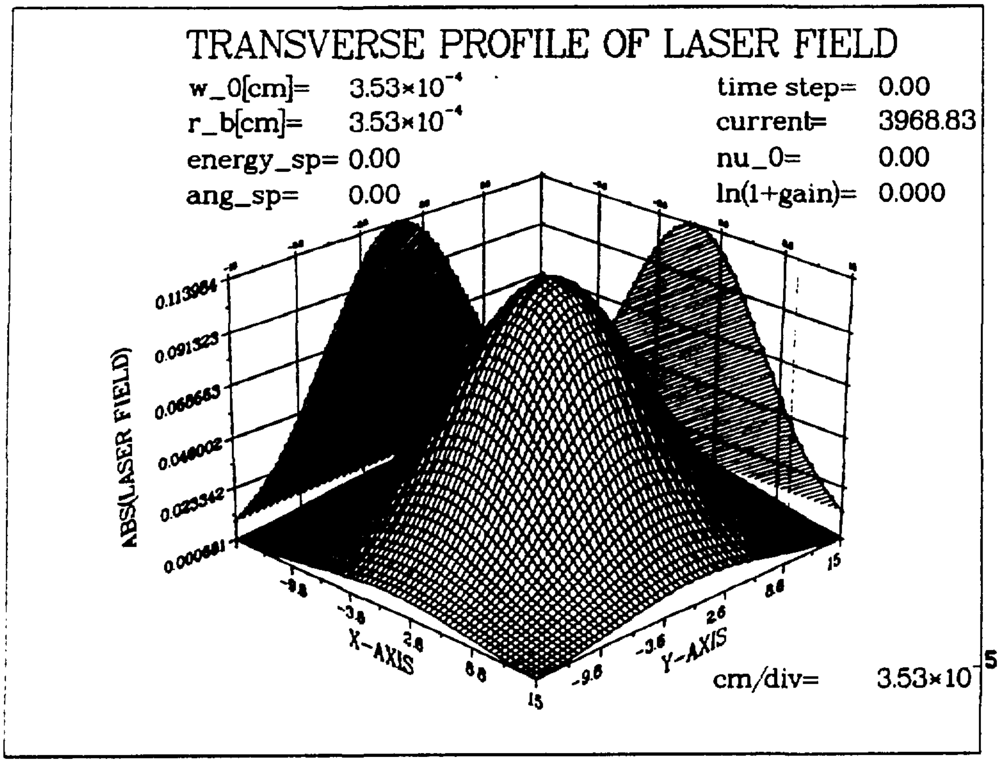
TRANSVERSE PROFILE OF LASER FIELD
w_0[cm]= 3.53×10^-4
r_b[cm]= 3.53×10^-4
energy_sp= 0.00
ang_sp= 0.00
time step= 0.00
current= 3968.83
nu_0= 0.00
ln(1+gain)= 0.000
ABS(LASER FIELD)
0.113984
0.091323
0.068663
0.046002
0.023342
0.000681
X-AXIS
Y-AXIS
-9.8
-3.6
2.6
8.8
15
cm/div= 3.53×10^-5

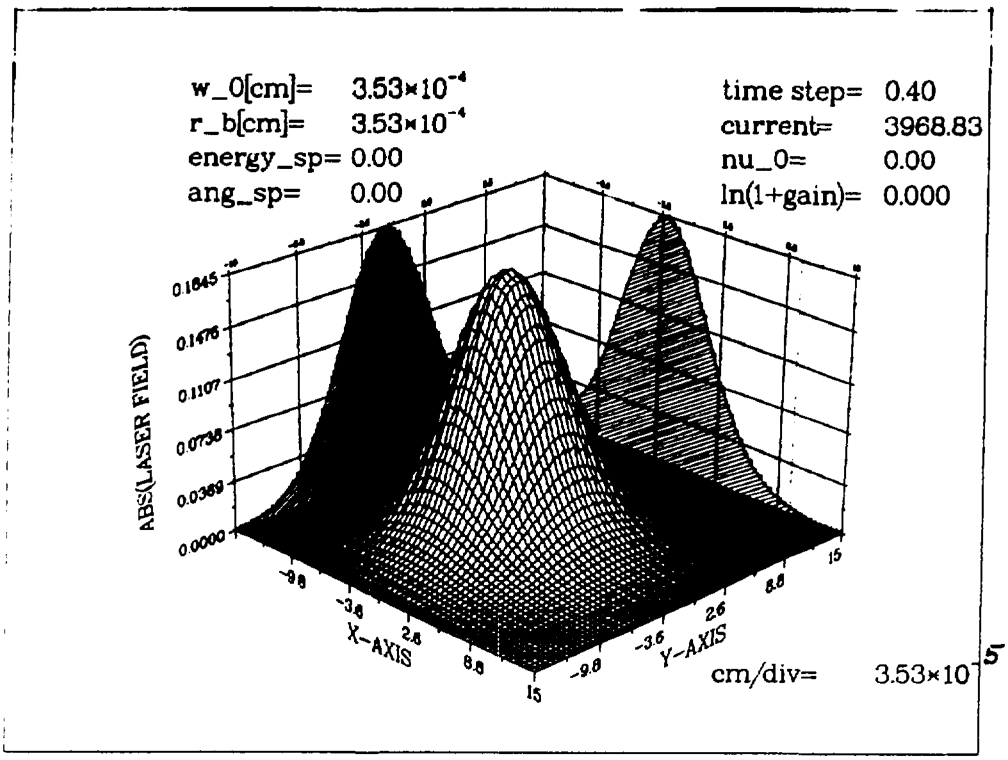
w_0[cm]= 3.53×10^-4
r_b[cm]= 3.53×10^-4
energy_sp= 0.00
ang_sp= 0.00
time step= 0.40
current= 3968.83
nu_0= 0.00
ln(1+gain)= 0.000
ABS(LASER FIELD)
0.1845
0.1476
0.1107
0.0738
0.0369
0.0000
X-AXIS
Y-AXIS
-9.8
-3.6
2.6
8.8
15
cm/div= 3.53×10^-5

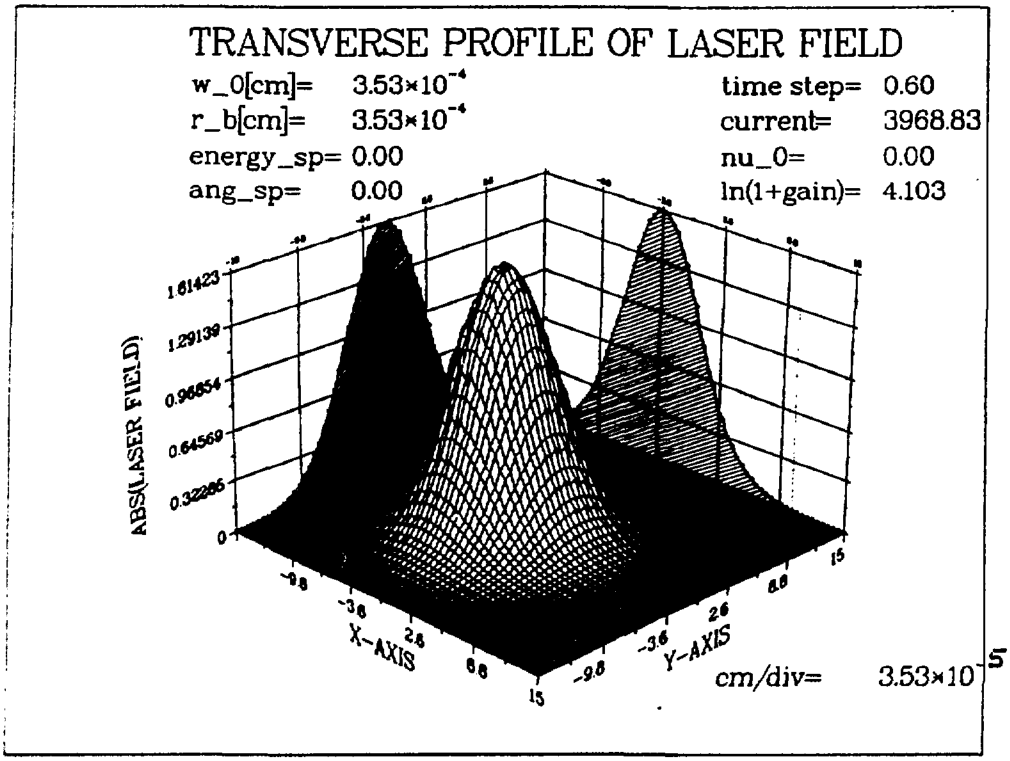
TRANSVERSE PROFILE OF LASER FIELD
w_0[cm]= 3.53×10^-4
r_b[cm]= 3.53×10^-4
energy_sp= 0.00
ang_sp= 0.00
time step= 0.60
current= 3968.83
nu_0= 0.00
ln(1+gain)= 4.103
ABS(LASER FIELD)
1.61423
1.29139
0.96854
0.64569
0.32285
0
X-AXIS
Y-AXIS
-9.8
-3.6
2.6
8.8
15
cm/div= 3.53×10^-5

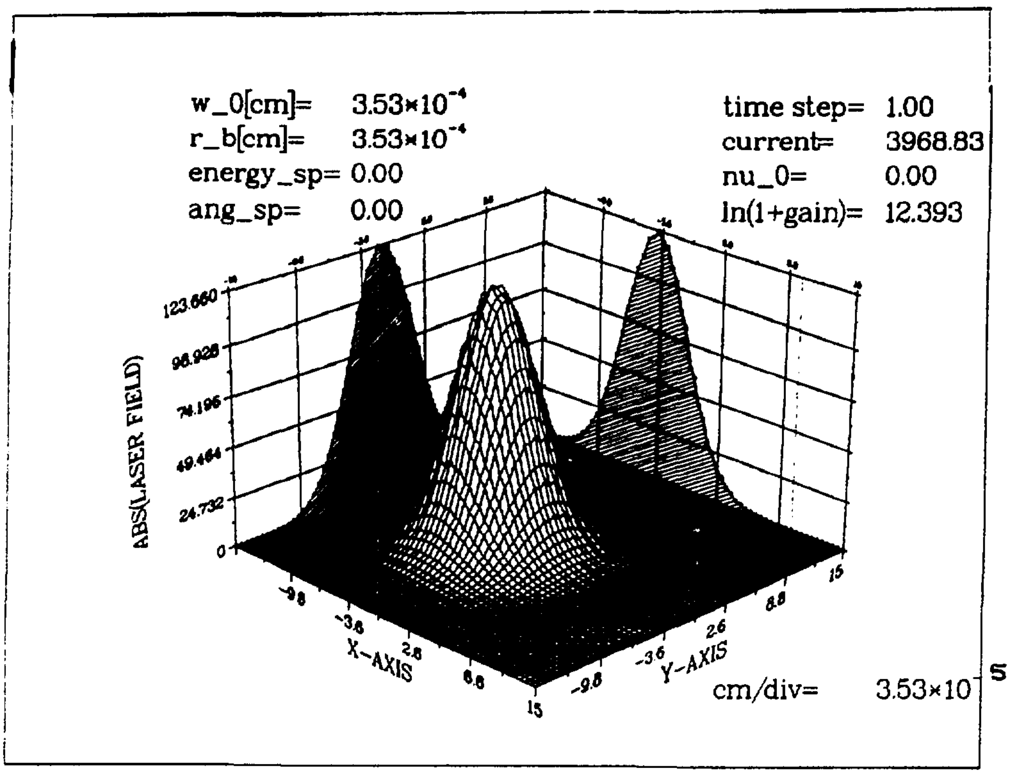
w_0[cm]= 3.53×10^-4
r_b[cm]= 3.53×10^-4
energy_sp= 0.00
ang_sp= 0.00
time step= 1.00
current= 3968.83
nu_0= 0.00
ln(1+gain)= 12.393
ABS(LASER FIELD)
123.660
98.928
74.196
49.464
24.732
0
X-AXIS
Y-AXIS
-9.8
-3.6
2.6
8.8
15
cm/div= 3.53×10^-5

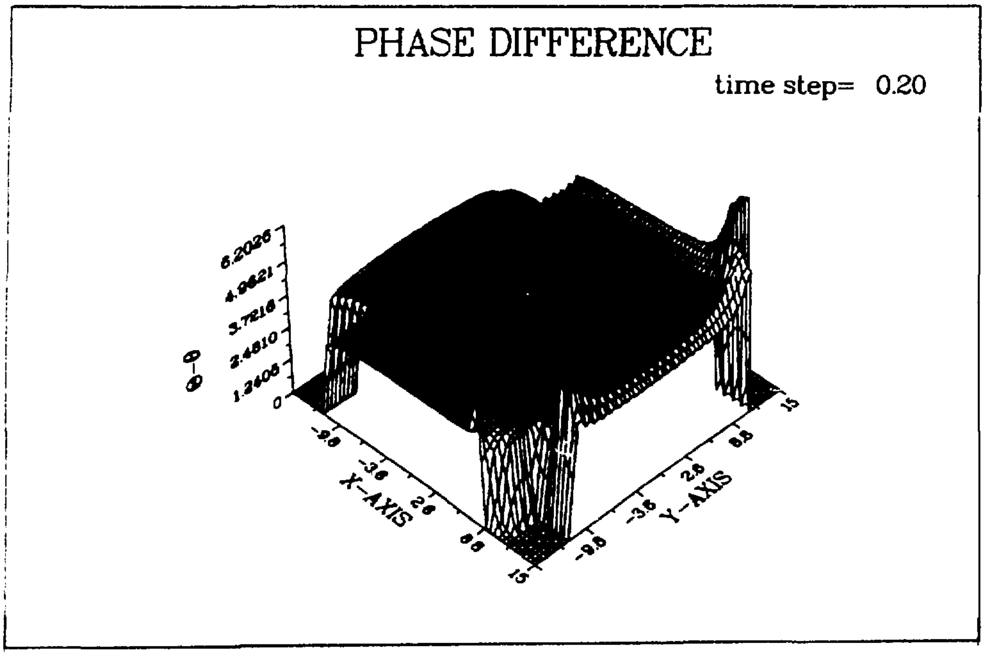
PHASE DIFFERENCE
time step= 0.20
6.2026
4.9621
3.7216
2.4810
1.2405
0
Θ−θ
-9.8
-3.6
2.6
8.8
15
X-AXIS
Y-AXIS

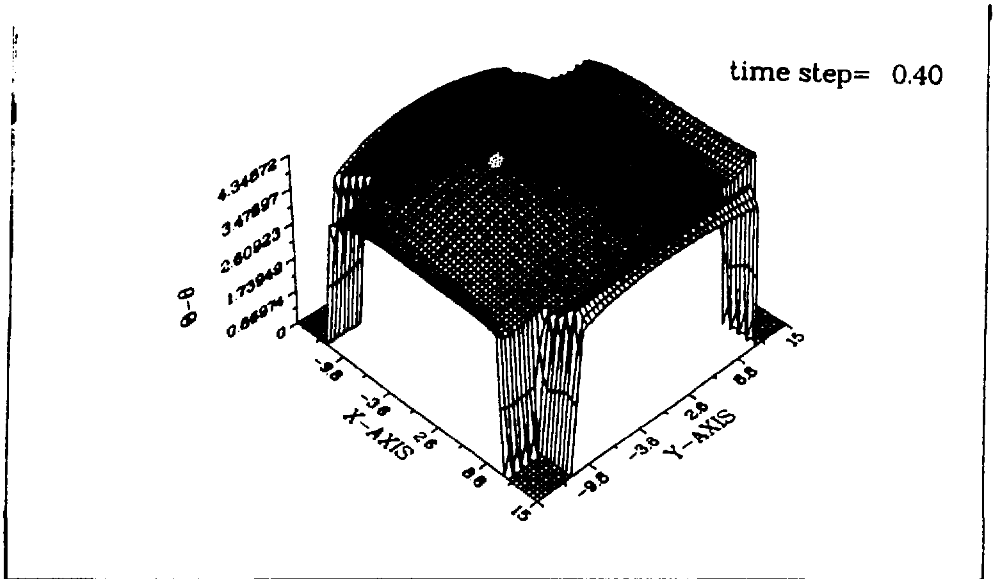
time step= 0.40
4.34872
3.47897
2.60923
1.73949
0.86974
0
Θ−θ
-9.8
-3.6
2.6
8.8
15
X-AXIS
Y-AXIS

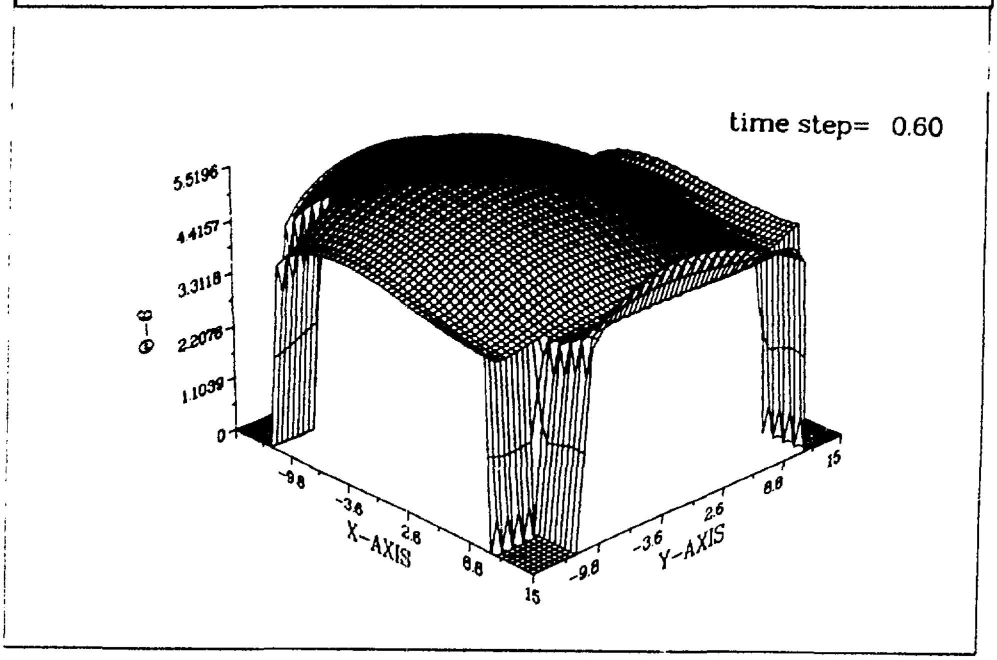
time step= 0.60
5.5196
4.4157
3.3118
2.2078
1.1039
0
Θ−θ
-9.8
-3.6
2.6
8.8
15
X-AXIS
Y-AXIS

PHASE DIFFERENCE

time step= 0.80

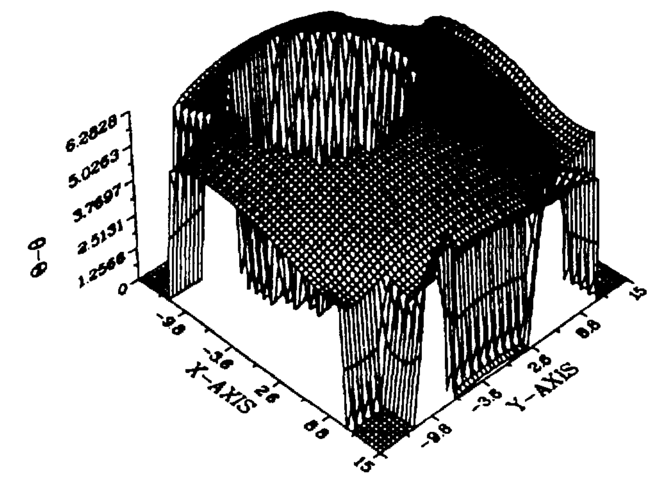

time step= 1.00

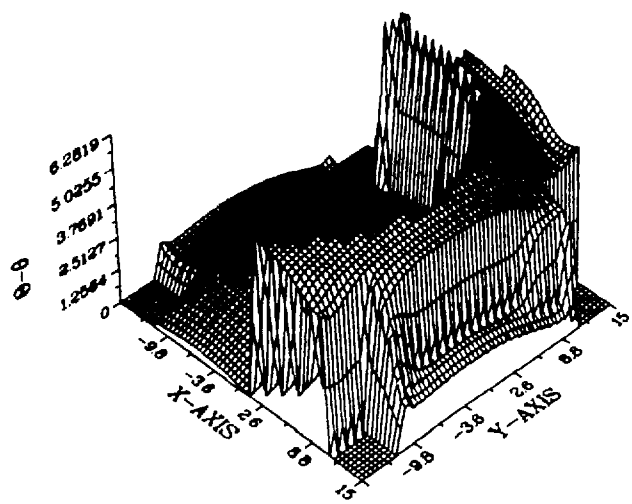

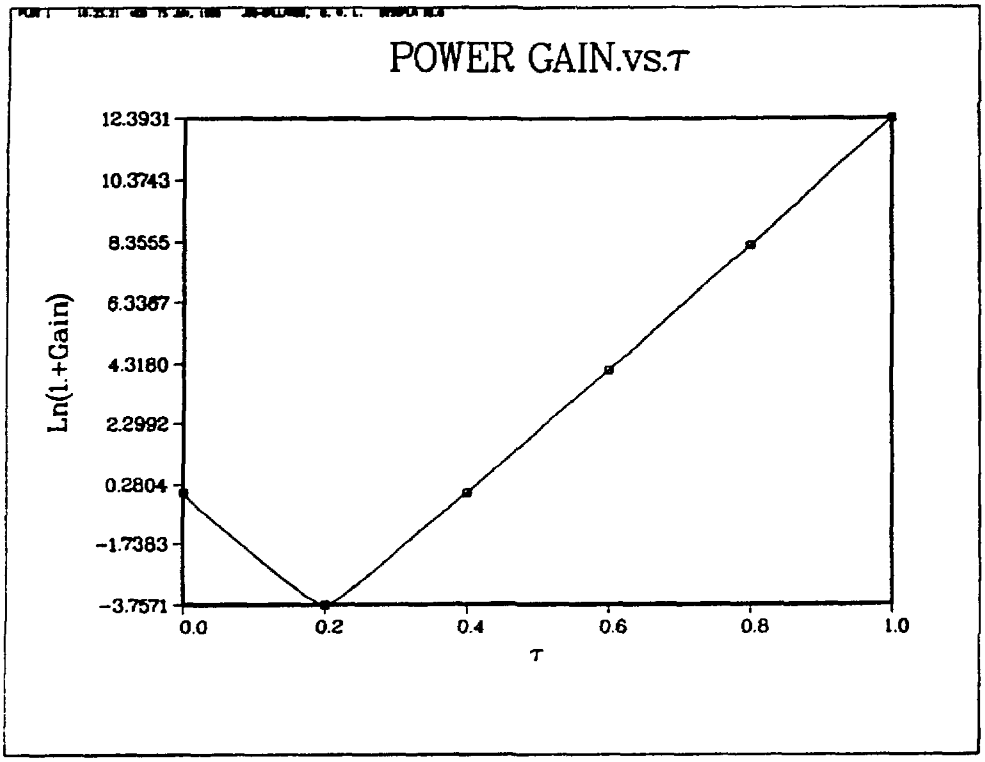
POWER GAIN.vs.τ
Ln(1.+Gain)
12.3931
10.3743
8.3555
6.3367
4.3180
2.2992
0.2804
-1.7383
-3.7571
0.0
0.2
0.4
0.6
0.8
1.0
τ

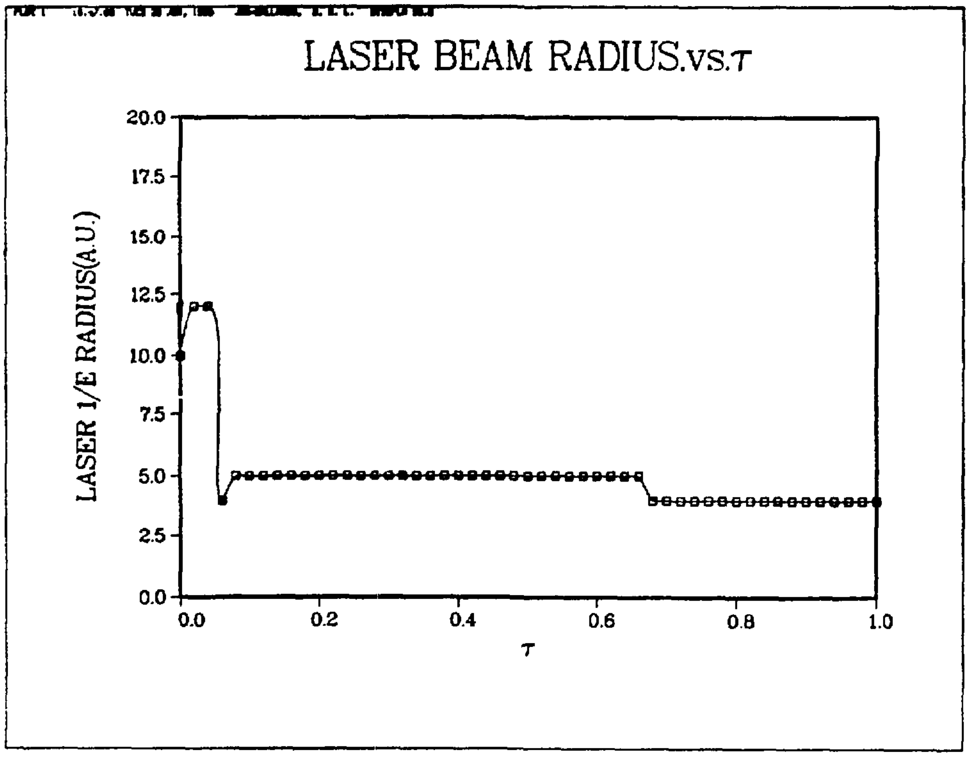
LASER BEAM RADIUS.vs.τ
LASER 1/E RADIUS(A.U.)
20.0
17.5
15.0
12.5
10.0
7.5
5.0
2.5
0.0
0.0
0.2
0.4
0.6
0.8
1.0
τ